Supporting Information

Real-Time Imaging of Metallic Supraparticle Assembly during Nanoparticle Synthesis

Mei Wang,[1] Chiwoo Park,[2] Taylor J. Woehl[1,*]

[1]Department of Chemical and Biomolecular Engineering, University of Maryland, College Park, MD

[2]Department of Industrial and Manufacturing Engineering, Florida State University, Tallahassee, FL

[*]Corresponding author, email: tjwoehl@umd.edu

Table of Contents

1. LP-TEM Experiments

Stock solutions of 20 mM potassium tetrachloroplatinate (K_2PtCl_4, Sigma-Aldrich, ≥ 99.99%, trace metals basis) and 10 mM sodium citrate (SC, $HOC(COONa)(CH_2COONa)_2 \cdot 2H_2O$, RICCA, ACS Reagent Grade) were prepared by dissolving salts in deionized water (18.2 MΩ) respectively. Tert-butanol (TBA, $(CH_3)_3COH$, Sigma-Aldrich, ≥ 99.5%) was combined with the stocks and additional water to prepare precursor solutions for LP-TEM experiments. Aqueous solutions (0.15 mM K_2PtCl_4 solution, 0.15 mM K_2PtCl_4 + 1 M TBA, and 0.15 mM K_2PtCl_4 + 1 M TBA + 1 mM SC) were degassed for 1 h by sonication (Bransonic, CPX2800H) prior to LP-TEM experiments. The LP-TEM experiments were performed on a Protochips liquid cell holder (Poseidon Select), which encloses a thin liquid layer by sandwiching liquid between two silicon chips, each having 550×50 μm free standing electron transparent 50 nm thick silicon nitride (SiN_x) membranes. One chip had 150 nm gold spacer posts to define the liquid thickness and channel. Prior to assembling the liquid cell, both chips were rinsed with acetone and methanol for two minutes each and then plasma cleaned for 3 min (Harrick Plasma, PDC-32G) to remove organic contamination and render the chip surfaces hydrophilic. The precursor was drop-cast (2 μL) onto the spacer chip and then the chips were sandwiched together and the holder tip sealed. Precursor solution was flowed between the two chips for 15 min using a syringe pump (Harvard Apparatus) with a flow rate of 300 μL/h to remove any bubbles or contamination. The liquid thickness was approximately 500 nm.[1] LP-TEM experiments were performed in a JEOL JEM-2100F Field Emission Gun (FEG) TEM operating at 200 kV in STEM mode with imaging magnification from 80 kx-200 kx, beam current from 21-107 pA, yielding dose rates from 0.5-17.9 MGy/s. Each experiment was performed along the edge of the window to keep the liquid thickness constant and each experiment was separated by 10 μm. In between each nanoparticle growth experiment,

precursor was flowed for 5 minutes at a flow rate of 300 μL/h to prevent depletion.[2, 3] *In situ* videos of supraparticle formation were generated by continuously scanning the STEM beam with Digital Micrograph (1024 × 1024 pixel, 5 μs dwell time at each pixel) and recording the screen (Camtasia studios, 10 frames/s). Videos were further analyzed by multi-object tracking analysis (See below). After the LP-TEM experiments, the SiN_x membranes coated in supraparticles were rinsed to remove excess precursor and air-dried. The morphology and structure of platinum nanocrystals and supraparticles were imaged with HRTEM.

2. Multi-Object Tracking Analysis (MOTA) For Tracking Sizes and Locations of Particles

An automated multi-object tracking algorithm (MOTA)[4] was applied to LP-TEM videos to automatically identify and track individual Pt particles. For each of the videos, the automated algorithm first identifies potential particle images for each image frame of the video using the iterative voting algorithm[5] to locate particle centers and exploit the center information to segment overlapped particle images into individual particle images. The algorithm then associates the particle images over different image frames based on their spatial proximities and geometrical similarities. During the association process, most faulty particle identifications are filtered out and mis-detected particles are additionally identified to improve the accuracy of analysis. The algorithm solves an optimization problem that maximizes the chances of the same particles being associated into same groups and each of the groups forms a trajectory of particle changes. Once the association is completed, the algorithm extracts the center locations and sizes of particles in the trajectories, which produces the trajectories of particle changes in locations and sizes.

3. Single Supraparticle Growth Kinetics

To ensure the accuracy of multi-object tracking analysis, only the growth kinetics of supraparticles with nucleation induction times < 40 s and initial radii < 10 nm were analyzed. We

found that supraparticles outside of this range had incomplete or erroneous MOTA data. To support that the supraparticle radius followed a cubic power law increase with time as shown in the main text, we also fit growth kinetic data to two other power laws corresponding to reaction limited (SE.3) and mixed diffusion and reaction control (SE.4):

$$t = mr_{supra}^{2} + t_0 \tag{SE.3}$$

$$a(r_{supra})^3 + b(r_{supra})^2 = t - t_0 \tag{SE.4}$$

Figure S1a shows that the model for reaction limited growth did not fit the growth data as well compared to the diffusion limited model. The mixed diffusion and reaction control equation accurately fit the data (**Figure S1b**), but nearly 80% of the fits yielded values of b that were < 0.

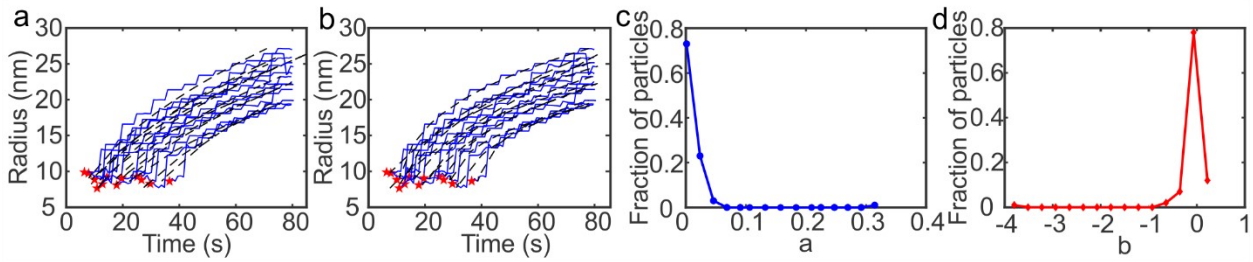

Figure S1. Platinum supraparticle radius as a function of time (solid blue lines) fit by non-linear least squares fits (black dashed lines) of equations SE.3 (a) and SE.4 (b). (c-d) Histograms of fitting constants a and b.

4. Interparticle Interaction Calculations

Interparticle interactions were calculated based on the interaction potential energy between two platinum spheres with radii of 1.5 nm. Each expression below was derived from expressions for two flat plates using the Derjaguin approximation. The Van der Waals interaction energy U_{VdW} between two spherical nanoparticles was calculated *via* the following equations,[6]

$$h_1 = \frac{S}{r_p} \tag{SE.5}$$

$$h_2 = \frac{S}{4r_p} \tag{SE.6}$$

$$h_3 = \frac{S^2}{4{r_p}^2} \tag{SE.7}$$

$$F_p = 1 - 0.0532 * S * 10^9 * In(1 + \frac{18.80}{S * 10^9}) \tag{SE.8}$$

$$U_{vdW} = -\frac{AF_p}{12h_1}\left\{\frac{1}{1+h_2} + \frac{h_1}{1+h_1+h_3} + 2h_1 * In\left[\frac{h_1(1+h_2)}{1+h_1+h_3}\right]\right\}. \tag{SE.9}$$

Here S is the surface-to-surface distance between two nanocrystals, F_p is the retardation correction factor, and $A = 3.132 \times 10^{-19} J$ is the Hamaker constant between two platinum nanoparticles separated by DI water at room temperature .[7] The steric interaction energy, U_{st}, causes interparticle repulsion due to adsorbed polymer on nanocrystal surfaces and can be calculated by the following expressions,[8]

for $l \leq S < 2l$:

$$U_{st} = \frac{4\pi r_p k_B T \emptyset^2 (0.5 - \chi)(l - \frac{S}{2})^2}{V_{m,\ water}}, \tag{SE.10}$$

for $S < l$:

$$U_{st} = \frac{4\pi r_p k_B T \emptyset^2 (0.5 - \chi) l^2}{V_{m,\ water}} \left(\frac{S}{2l} - 0.25 - In\frac{S}{l} \right).$$

(SE.11)

Here l is the polymer coating thickness (estimated as 1 nm), $\emptyset$ is the ligand volume fraction (estimated to be 0.5), χ is the Flory-Huggins parameter (estimated to be 0 for favorable ligand-solvent interactions), and $V_{m,\ water}$ is the molecular volume of water.

When citrate ions are present, they adsorb to platinum nanoparticle surfaces because they are chelating agents, which causes interparticle repulsion between charged citrate groups on the neighboring nanoparticle surface. The repulsive electrostatic interparticle interaction can be estimated by,[8]

$$U_{ele} = \frac{32\pi\epsilon {k_B}^2 T^2 r_p}{z^2 e^2} tanh\left(\frac{ez\psi_s}{4k_B T}\right)^2 \exp\left(-\kappa S\right).$$

(SE.12)

Here ϵ is the absolute permittivity of water, z is the counterion valence (z = 1 for potassium ions), e is the elementary electric charge, ψ_s is the surface potential on the platinum nanocrystals (estimated to be -35 mV),[9, 10] and κ is the Debye parameter,

$$\kappa = \sqrt{\frac{2N_A e^2 I_s}{\epsilon k_B T}}, \qquad \text{(SE.13)}$$

where N_A is the Avogadro's number and I_s is the ionic strength of the solution in mol/L.

5. Electron energy loss spectroscopy of supraparticles

Electron energy loss spectroscopy (EELS) was performed at 200 kV electron energy in STEM imaging mode using a Gatan Image Filter (GIF) with the dispersion set to 0.03 eV/pixel. Carbon K-edge spectra were acquired from the supraparticles (inset Figure S2a) and SiN membrane, each with a total exposure time of 45 seconds. An exponential background was fit to the raw EELS spectrum from 265-280 eV and subtracted from the raw spectrum to produce the carbon K-edge spectra (Figure S2b).

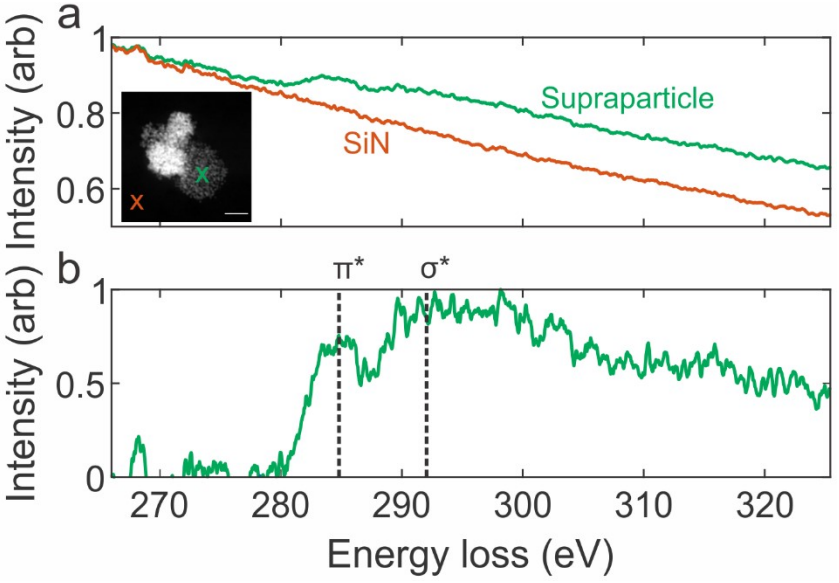

Figure S2. Core-loss electron energy loss spectroscopy (EELS) of a platinum supraparticle shows carbon within the particle. (a) Raw core law EELS of the carbon K-edge (~280 eV energy loss) from a spot within the supraparticle (green) and on the silicon nitride substrate (orange). (b) Background subtracted EELS data of the carbon K-edge. Dashed lines denote the energies associated with each carbon bonding mode. The spectral shape indicates the carbon is amorphous.

References

1. Wang, M.; Park, C.; Woehl, T. J. *Chemistry of Materials* **2018,** 30, (21), 7727-7736.
2. Moser, T. H.; Mehta, H.; Park, C.; Kelly, R. T.; Shokuhfar, T.; Evans, J. E. *Science Advances* **2018,** 4, (4), eaaq1202.
3. Abellan, P.; Woehl, T. J.; Parent, L. R.; Browning, N. D.; Evans, J. E.; Arslan, I. *Chemical Communications* **2014,** 50, (38), 4873-4880.

4. Park, C.; Woehl, T. J.; Evans, J. E.; Browning, N. D. *IEEE Transactions on Pattern Analysis and Machine Intelligence* **2015,** 37, (3), 611-624.
5. Parvin, B.; Yang, Q.; Han, J.; Chang, H.; Rydberg, B.; Barcellos-Hoff, M. H. *IEEE Transactions on Image Processing* **2007,** 16, (3), 615-623.
6. Hunter, R. J., *Foundations of colloid science*. 2nd ed. ed.; Oxford University Press: Oxford ;, 2001.
7. Tolias, P. *Surface Science* **2020,** 700, 121652.
8. Fritz, G.; Schädler, V.; Willenbacher, N.; Wagner, N. J. *Langmuir* **2002,** 18, (16), 6381-6390.
9. Drzymała, E.; Gruzeł, G.; Pajor-Świerzy, A.; Depciuch, J.; Socha, R.; Kowal, A.; Warszyński, P.; Parlinska-Wojtan, M. *Journal of nanoparticle research : an interdisciplinary forum for nanoscale science and technology* **2018,** 20, (5), 144.
10. Lebedová, J.; Hedberg, Y. S.; Odnevall Wallinder, I.; Karlsson, H. L. *Mutagenesis* **2017,** 33, (1), 77-85.